https://doi.org/10.5194/egusphere-2026-1603
Preprint. Discussion started: 18 May 2026

Mechanisms and Patterns of Snow–Temperature Interactions in Arid Mountains: Coupling Coordination and Lagged Responses Across Xinjiang, China

Haixing Li*[1], Xiaolong Bao[1], Shiqi Lu[1], Yi Chu[2], Jun Lu[1], Mengge Xiao[1], Xuelei Lei[1]

[1]College of Geomatics Science and Technology, Nanjing Tech University, Nanjing 211816, China;

[2]Xinjiang Key Laboratory of Water Cycle and Utilization in Arid Zone, Xinjiang Institute of Ecology and Geography, Chinese Academy of Sciences 830011, Urumqi, China

Correspondence to: Haixing Li (leehaixing@126.com)

https://doi.org/10.5194/egusphere-2026-1603
Preprint. Discussion started: 18 May 2026

Abstract. The interaction between snow depth (SD) and land surface temperature (LST) is a critical yet underexplored process in arid mountain hydrology. This study introduces an integrated analytical framework combining Coupling Coordination Degree Model (CCDM) and time-lagged correlation analysis to systematically quantify the interaction strength, synergistic quality, and dynamic response times between SD and LST across the complex mountain-basin systems of Xinjiang, China. Using long-term, high-resolution remote sensing data, we reveal a hierarchical control system governing snow–temperature interactions: macro-scale latitudinal climate divides establish a north–south contrast in coupling potential; meso-scale topography overrides this pattern in southern mountains, where elevation becomes the dominant control on coupling and coordination; and micro-scale local factors drive east–west divergences in response lags. Key findings include: (1) pronounced north–south asymmetry in the Tianshan Mountains, with the sensitive south slope showing significant spring lag lengthening; (2) elevation-dependent thresholds in the Kunlun Mountains, where snow–temperature coordination improves only above 3500 m; and (3) region-specific lag dynamics indicating altered snowpack thermal inertia (e.g., prolonged spring lags in the Tianshan) and memory effects. The discrepancy between coupling degree and coordination degree emerges as a key diagnostic, identifying vulnerable regions where strong temperature forcing is mismatched with sustainable snowpack evolution. This study provides a process-aware framework that moves beyond statistical correlation, offering quantitative metrics to improve the representation of mountain snow–climate feedbacks in hydrological and climate models under accelerating warming.

1 Introduction

Snow, a critical component of the global cryosphere, significantly influences Earth's climate system through its distinct radiative and thermodynamic properties, including high surface albedo, low thermal conductivity, and latent heat exchange during phase transitions (Essery, 2013; Smith and Barstad, 2004) . These properties establish snow as a key interface in land–atmosphere interactions, regulating surface energy budgets, modulating hydrological cycles, and contributing to regional climate feedback mechanisms. While snow cover extent provides a broad indicator of climatic variability (Barnett et al., 2005), snow depth serves as a more precise and dynamically meaningful variable, integrating the net effects of accumulation and ablation over time. As a fundamental state parameter in snow hydrology, it captures the cumulative response to meteorological forcing and snowpack evolution, making it essential for climate modeling, runoff forecasting, and ecological assessment (Liston and Elder, 2006; Raleigh et al., 2015). Consequently, quantifying the spatiotemporal dynamics of snow depth is crucial for predicting water availability, assessing climate change impacts, and supporting adaptation strategies in snow-dominated regions.

The Xinjiang Uygur Autonomous Region is a hydrologically critical zone in arid Central Asia, encompassing a unique mountain–basin system comprising the Altai, Tianshan, and Kunlun ranges, along with the intervening Junggar and Tarim

https://doi.org/10.5194/egusphere-2026-1603
Preprint. Discussion started: 18 May 2026

Basins (Chen et al., 2015) . This configuration creates a natural laboratory with pronounced climate, topographic, and snow accumulation gradients (Zhang et al., 2019). The region's water security is fundamentally dependent on snowmelt from these high mountains. However, the mechanistic responses of snowpack dynamics to thermal forcing—particularly across different mountain ranges and elevation zones—remain poorly quantified at process-relevant scales. The complex interplay between continental climate and extreme topography generates heterogeneous interactions that challenge existing models (Li et al., 2020; Wang et al., 2022).

Snowpack evolution is governed by the coupling effects of radiative, thermal, and mass exchange processes, with land surface temperature (LST) playing a predominant role by directly modulating sensible and latent heat fluxes (Lehning et al., 2002a, b; Male and Gray, 1981; Marks and Dozier, 1992; Pomeroy et al., 1998) . Extensive evidence from remote sensing and modeling has established LST as a key explanatory variable for snow depth variability worldwide, a linkage underscored by major synthesis reports (Arias et al., 2021; López-Moreno et al., 2013; Musselman et al., 2017).

However, this relationship is characterized by substantial complexity—non-linearities, hysteresis, and strong spatiotemporal heterogeneity (Beniston et al., 2018) . Interactions involve both immediate thermodynamic adjustments and lagged hydrological feedbacks that vary systematically with elevation, season, and regional climate. For instance, in the Tianshan Mountains, warming has led to reduced snow duration, delayed accumulation, and faster melt (Aizen et al., 2007). Critically, accounting for temporal lags significantly enhances the observed correlation, revealing memory effects within the snowpack (Hock and Holmgren, 2005). Furthermore, the dominant thermal driver is not static but can shift across ablation phases, as seen in the central Tianshan where surface temperature initiates melt while air temperature governs peak ablation (Li et al., 2022). These elevation-dependent and seasonally variable patterns, echoed in other major mountain ranges (Immerzeel et al., 2010; Marty et al., 2017), collectively highlight those conventional correlative approaches are ill-equipped to quantify the coupling coordination state and capture the time-lagged synergy between snow depth and temperature.

These specific shortcomings stem from the prevailing analytical paradigm that relies on statistical correlations. While robustly establishing empirical relationships, this approach harbors two fundamental limitations (Clark et al., 2011). First, it treats snow and temperature as separate but co-varying quantities, failing to capture their intrinsic coupling and synergistic evolution. Second, it largely overlooks the temporal dimension of interaction, specifically the time-lagged response, which is essential for mechanistic understanding and hydrological prediction. Consequently, key questions remain unanswered: How is the strength of snow–temperature interaction spatially organized? Does a strong correlation imply a healthy, coordinated co-evolution? Over what time scales does snowpack adjust to thermal forcing across different terrains and seasons? The lack of a coherent framework to systematically diagnose both the strength of coupling and the quality of coordination, while accounting for time-lagged synergy, constitutes a major obstacle to improving process representation in models (Nijssen et al., 2001).

To address this gap, this study develops and applies an integrated analytical framework combining coupling coordination theory with time-lag modeling to systematically investigate the interactive relationship between snow depth and land surface

https://doi.org/10.5194/egusphere-2026-1603
Preprint. Discussion started: 18 May 2026

temperature across Xinjiang. Utilizing long-term, high-resolution remote sensing data, we quantify three fundamental aspects: (1) the degree of coupling; (2) the coordination level across climatic seasons and topographic settings; and (3) the spatiotemporal patterns of response time lags.

This investigation makes three primary contributions to cryospheric science: First, it establishes a quantitative, process-informed understanding of how snowpack responds to thermal forcing across one of Central Asia's most hydrologically critical regions. Second, it introduces and validates an analytical framework—combining coupling, coordination, and lag analysis—that can be applied to other snow-dominated regions globally. Third, it provides empirically derived parameters and relationships that can directly improve the physical representation of snow processes in regional climate and hydrological models. By bridging the gap between statistical correlation and mechanistic understanding, this work advances our capacity to predict snowpack responses to ongoing climate change, with direct implications for water resource management, ecosystem conservation, and climate adaptation planning in Xinjiang and analogous snow-dependent regions worldwide.

2 Study area and Data introduction

2.1 Study area

The Xinjiang Uygur Autonomous Region (73°40′E–96°18′E, 34°25′N–48°10′N) encompasses approximately 1.66 million km² in the arid interior of Eurasia. Its terrain is organized into a distinct sequence of six north–south oriented units: the Altai Mountains(N1), Junggar Basin (N2), northern and southern Tianshan Mountains (N3 and S1), Tarim Basin (S2), and Kunlun Mountains (S3) (Fig. 1). This configuration drives extreme contrasts in climate—from the humid alpine zones of the northern mountains to the hyper-arid Tarim Basin—and creates corresponding gradients in snow accumulation and persistence. The regional snowline elevation reflects this variability, ranging from ~3,200 m in the Altai to 3,230–4,290 m in the Tianshan (Hu, 2004). As a region containing roughly one-third of China's snow water resources (Marchane et al., 2015; Xuezhi et al., 2000), Xinjiang provides an ideal setting for examining snow–climate interactions across pronounced environmental gradients.

To systematically examine how snow depth (SD) and land surface temperature (LST) respond differently across contrasting climatic and topographic settings, we delineated the TianShan Mountains into northern and southern slope units based on the mountain ridge line. The northern slope falls within the mid-temperate arid zone of northern Xinjiang, whereas the southern slope belongs to the warm-temperate arid zone of southern Xinjiang. This division, combined with the broader regional classification, resulted in six distinct geographical-climatic units used for subsequent comparative analysis (Fig. 1).

https://doi.org/10.5194/egusphere-2026-1603
Preprint. Discussion started: 18 May 2026

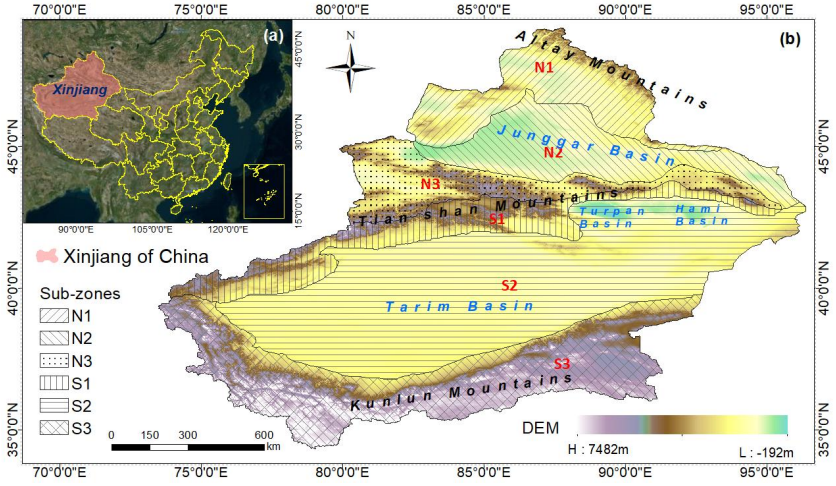

Figure 1. Map of the study area. (a) Location of Xinjiang Uygur Autonomous Region in China (satellite base map obtained from Tianditu, National Geospatial Information Service Platform of China, https://www.tianditu.gov.cn/).(b) The six sub-regions of Xinjiang that constitute the study area (drawn by the author).

2.2 Data source

2.2.1 Downscaled snow depth (SD) dataset

We used a high-resolution daily snow depth dataset, which was downscaled to 500 m spatial resolution and processed to remove cloud obscuration. This long-term, continuous series was developed by the authors, with the detailed production methodology and validation procedures fully documented at the National Cryosphere Desert Data Center of China. The dataset is publicly accessible under the same reference.

2.2.2 Land surface temperature (LST) data

Land surface temperature (LST) data were obtained from the Thermal and Reanalysis Integrating Moderate-resolution Spatial-seamless (TRIMS) LST dataset, available through the National Tibetan Plateau Data Center. This dataset integrates Terra/Aqua MODIS LST products and Global Land Data Assimilation System (GLDAS) data, with supplementary variables including satellite-derived vegetation indices and surface albedo. The TRIMS reconstruction method combines high-frequency and low-frequency LST components with spatial correlation information from thermal infrared remote sensing and reanalysis sources to generate a gap-free, all-weather LST product at 1 km spatial resolution and twice-daily temporal resolution. To ensure consistency with the snow depth dataset, daily mean LST values were computed from morning and evening overpasses and spatially resampled to a uniform 500 m grid.

https://doi.org/10.5194/egusphere-2026-1603
Preprint. Discussion started: 18 May 2026

3 Methodologies

3.1 Coupling Coordination Degree Model

The concept of coupling, derived from physics, describes the phenomenon of mutual influence and interaction between two or more systems (Song et al., 2020). Building upon this, the notion of coupling coordination expands the framework to represent how systems can co-evolve toward a more ordered, synergistic state (Song et al., 2020). This approach has been effectively adapted to study interdependent systems across various fields, including ecology, geography, and economics (Lai et al., 2020; Zhao et al., 2025).

The Coupling Coordination Degree Model (CCDM) is an analytical framework that quantifies such relationships through two key metrics: the Coupling Degree (CD) and the Coupling Coordination Degree (CCD) (Huang et al., 2020; Liu et al., 2005). The CD measures the strength of association and mutual influence between systems, while the CCD further assesses the degree to which their development is harmonized. In this study, we apply the CCDM to analyze the interaction between snow depth (SD) and land surface temperature (LST). The Coupling Degree (CD) is calculated as follows:

$$C = \left[\frac{S \times E}{[(S+E)/2]^2}\right]^{\frac{1}{2}} \quad (1)$$

Where, S and E represent the SD and LST, respectively, while C stands for the coupling degree, indicating the intensity of interaction between the two systems. the larger the value, the better the system development.

The CD indicates the interaction intensity between subsystems like SD-LST, it fails to assess their coordinated development (Huang et al., 2020). To quantify this coordination, CCD is introduced, which evaluates both interaction magnitude and mutual promotion/restraint. The calculation method is as follows:

$$T = \alpha \cdot S + \beta \cdot E \quad (2)$$

$$D = (C \times T)^{\frac{1}{2}} \quad (3)$$

Where, D denotes the CCD, ranging from 0 to 1; higher values indicate greater coordinated development of the SD-LST system. T represents the comprehensive evaluation index reflecting subsystem contributions. α and β (both set at 0.5 here) signify subsystem interaction weights. CD and CCD are classified via Meng et al.'s (2024) and Zhang et al.'s(2023) standards (Table 1).

Table 1 Classification of coupling degree and coupling coordination degree.

CD	Coupling stage	CCD	Coupling coordination type	Classification
0	No coupling	0-0.2	Severe maladjustment recession	Misalignment recession interval
0-0.3	Primary coupling	0.2-0.4	Moderate maladjustment recession	
0.3-0.5	Antagonistic stage	0.4-0.5	Near maladjustment recession	
0.5-0.8	Break-in stag	0.5-0.6	Critical coordinated development	Coordinated

https://doi.org/10.5194/egusphere-2026-1603
Preprint. Discussion started: 18 May 2026

0.8-1	High-quality coupling	0.6-0.8	Primary coordinated development	development interval
1	Optimal stage	0.8-1.0	High quality coordination development	

3.2 Time-Lagged Cross-Correlation Analysis

To quantify the time-lagged relationships between snow depth (SD) and land surface temperature (LST), we employed a time-lagged cross-correlation approach (Wasserman, 2004). This method extends conventional autocorrelation analysis by measuring the linear association between two time series at different temporal offsets (lags), thereby capturing both instantaneous and delayed interactions. The model is applicable in bivariate settings and can be extended to multivariate contexts to account for lagged effects within coupling systems.

In this study, we apply this approach to characterize the dynamic interplay between SD and LST, specifically to identify the time lag at which their correlation is strongest and to evaluate the direction and magnitude of lagged responses. The cross-correlation coefficient R between SD and LST across varying time lags is computed as follows:

$$R_k(X,Y) = \frac{\sum_{i=1}^{n-k}(X_i-\overline{X_i})(Y_{i+k}-\overline{Y_{i+k}})}{\sqrt{\sum_{i=1}^{n-k}(X_i-\overline{X_i})\cdot\sum_{i=1}^{n-k}(Y_{i+k}-\overline{Y_{i+k}})}} \quad (4)$$

Where, $R_k(X,Y)$ denotes the correlation coefficient sequence between LST (X_i) and SD (Y_i) at lag k, where n is the sequence length and $k \in [0, n/4]$ (empirically determined). At k=0, SD responds instantaneously to LST, indicating synchronized evolution. The formula for computing the maximum cross-correlation coefficient and corresponding lag time for each k is as follows:

$$R_1(k_1) = \max\left(R_k(X,Y)\right) \quad (5)$$

$$R_2(k_2) = \min\left(R_k(X,Y)\right) \quad (6)$$

$$\begin{cases} R = R_1 & K = k_1 & |R_1| > |R_2| \\ R = null & K = null & |R_1| = |R_2| \\ R = R_2 & K = k_2 & |R_1| < |R_2| \end{cases} \quad (7)$$

Where, R_1 denotes the maximum correlation coefficient between SD and LST at lag k_1, while R_2 is the minimum at k_2. R and K represent the peak cross-correlation coefficient and corresponding lag time, respectively. Lag time categories are: K=0 (fastest, no delay), $1 \le K \le 7$ (fast), $8 \le K \le 14$ (medium), and $14 \le K \le 23$ (slow). Shorter lags indicate faster SD response to LST, with zero lag implying instantaneous response.

4 Results

4.1 Spatial-Temporal Patterns of SD and LST across Xinjiang

Figure 2 shows the interannual variations of annual average snow depth (SD) and land surface temperature (LST) across six sub-regions of Xinjiang over the 20-year study period. The 20-year mean SD (Fig. 2a) exhibits marked spatial heterogeneity, with deeper snowpacks predominantly located in the northern regions, where N1 records the highest regional mean of

https://doi.org/10.5194/egusphere-2026-1603
Preprint. Discussion started: 18 May 2026

approximately 6 cm. Overall, snow accumulation is most pronounced in the northern zones (N1, N3, N2) and the southern alpine area (S3), showing a clear north-to-south gradient. Maximum accumulation occurs on the northern slopes of the Tianshan Mountains (N3), while N2 maintains an average SD of 3.5 cm, exceeding values observed in the Kunlun Mountains(S3). In contrast, the Tarim Basin (S2) remains largely snow-free throughout most of the year. Decadal analysis reveals divergent trends: N1, N2, N3 and S1 show gradual declines in SD, while S2 and S3 exhibit slight but persistent increases.

Temporal trends of LST show differentiated variations across the six sub-regions (Fig. 2b). The highest mean annual LST values (>30°C) occur in the arid Tarim Basin (S2), followed by the Junggar Basin (N2, >25°C). The remaining mountain-dominated regions (S1, S3, N1, N3) maintain moderate LST regimes ranging between 10-18°C. Temporal analysis indicates a consistent warming trend across all regions except S2, with interannual variability particularly pronounced in the mountainous zones. These spatially differentiated patterns in both SD and LST provide critical context for investigating their interactive relationships through coupling coordination and time-lag analyses.

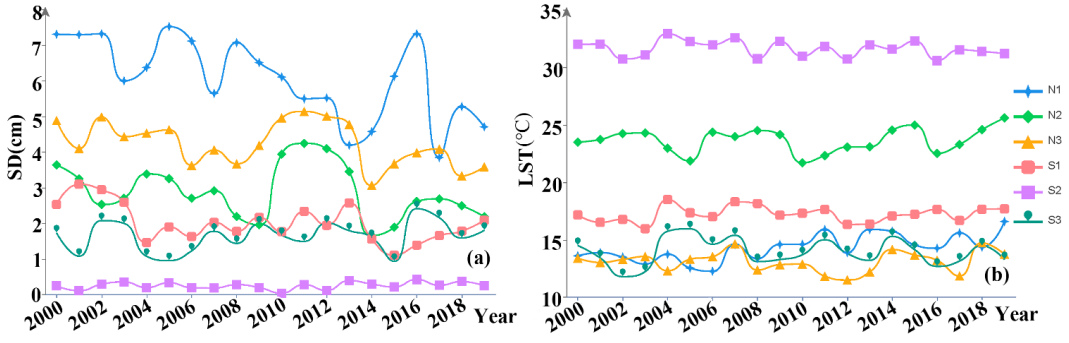

Figure 2. Twenty-year trends of SD and LST for each of the six sub-regions. (a) Sub-regional trends of SD; (b) Sub-regional trends of LST.

Scatter plot analyses were conducted to quantify the relationship between SD and LST across the six sub-regions (Fig. 3). Each panel displays the scatter distribution, linear regression fit, 95% confidence interval (shaded band), coefficient of determination (R^2), and Spearman's rank correlation coefficient (ρ). In five of the six sub-regions (N1, N2, N3, S1, and S3), both Spearman's ρ and R^2 indicate statistically significant negative correlations ($p < 0.01$ for ρ; R^2 ranging from 0.49 to 0.76, all $p < 0.001$). The majority of data points fall within the confidence intervals, supporting the robustness of the inverse relationship. In contrast, no significant correlation is observed in S2 (Tarim Basin): $\rho = -0.0011$ ($p \approx 1.0$) and $R^2 \approx 0$ ($p \approx 0.98$), indicating no linear or monotonic relationship between SD and LST due to limited seasonal snow cover and persistently high LST.

https://doi.org/10.5194/egusphere-2026-1603
Preprint. Discussion started: 18 May 2026

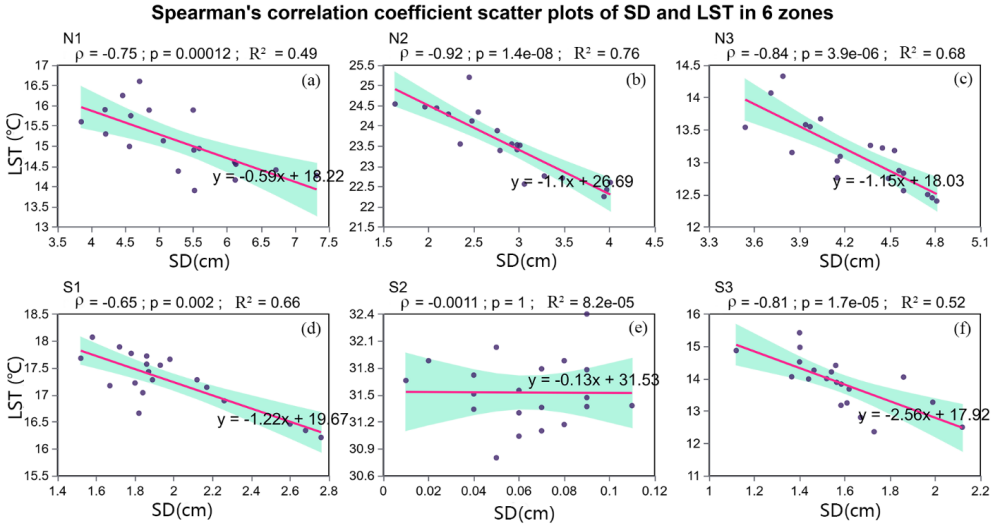

Figure 3. Spearman's rank correlation (ρ) and linear regression (R^2) between SD and LST for the six sub-regions over 20 years. Each subplot represents one sub-region, with ρ, p-value, and R^2 indicated.

These results demonstrate that in snow-abundant regions of Xinjiang, SD is consistently negatively correlated with LST, though the strength of this relationship varies spatially. However, correlation alone does not elucidate the directionality, lagged responses, or synergistic interactions between the two variables. This highlights the necessity of employing more nuanced analytical frameworks—such as coupling coordination and time-lag models—to better characterize the underlying SD–LST interaction mechanisms across different geographical and climatic contexts.

4.2 Coupling and Coordination Characteristics of SD–LST Interactions

4.2.1 Coupling Dynamics Between SD and LST

As illustrated in Fig. 4a, the spatial distribution of SD–LST coupling degree across Xinjiang over the 20-year period can be categorized into four types: Primary, Antagonistic, Break-in, and High-quality coupling. The northern regions (N1, N2, and N3) are predominantly characterized by High-quality coupling and the Break-in stage, reflecting strong snow–temperature interaction. However, the central and eastern parts of N2 and N3 exhibit notably lower coupling degrees, primarily classified as Antagonistic or Primary types. To the east of N2, coupling generally transitions further toward lower levels. In southern Xinjiang, the coupling degree in the S1 and S3 regions exhibits a clear elevational gradient: lower elevation zones are primarily in the Primary or Antagonistic stage, shifting progressively to Break-in and ultimately High-quality coupling with increasing altitude. In contrast, low-lying areas across all sub-basins consistently show low coupling levels, while most of the arid Tarim Basin (S2) remains in a low-coupling state throughout the study period.

https://doi.org/10.5194/egusphere-2026-1603
Preprint. Discussion started: 18 May 2026

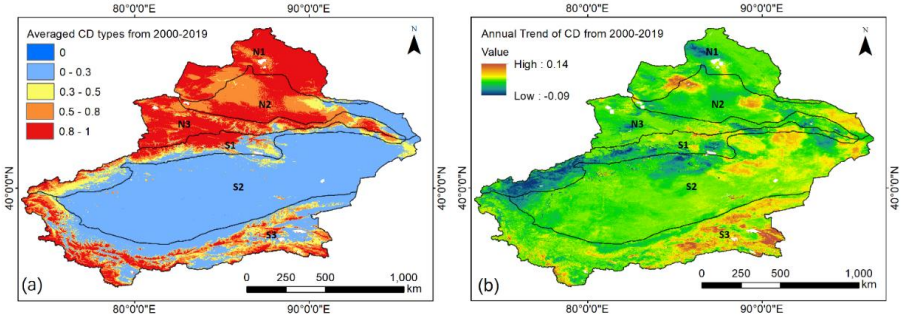

Figure 4. Distribution of average annual SD-LST Coupling types (see Table 1 for type definitions) and their 20-year changing trends, with (a) showing type distribution and (b) showing changing trends.

Spatiotemporal trends in the CD between SD and LST are shown in Fig. 4b. Over the study period, most regions exhibited minimal interannual fluctuation in CD. A discernible decreasing trend was observed in the lower-altitude southern slopes of the Altai Mountains (N1), the western Tianshan Mountains (western S1), and localized areas of the northern Tianshan (S2). In contrast, increasing CD trends occurred in scattered patches, primarily in the eastern sectors of N1, N2, S2, and S3, with the most pronounced strengthening evident in eastern S3.

In summary, the spatial coupling between SD and LST weakens from north to south across Xinjiang's mountain systems. The Altai Mountains (N1) maintained a consistently high and stable CD. Within the Tianshan ranges, CD values were significantly higher in the north than in the south, with a clear elevational gradient in the southern Tianshan and Kunlun Mountains, where CD increases with altitude. A notable decline was observed in the western Tianshan, whereas the eastern Kunlun Mountains showed a gradual strengthening of coupling over time.

Figure 5 illustrates the relationship between CD and altitude across the six sub-basins in Xinjiang. In the Altai Mountains (N1), CD remains consistently within the High-quality coupling category across all elevations, exhibiting a non-linear pattern that increases to a peak between 2700–3800 m before declining slightly at higher altitudes. Similarly, the Tianshan northern slope region (N3) maintains high CD values, though it displays a subtle decrease at mid-elevations (1600–2700 m), followed by a gradual recovery toward higher elevations.

https://doi.org/10.5194/egusphere-2026-1603
Preprint. Discussion started: 18 May 2026

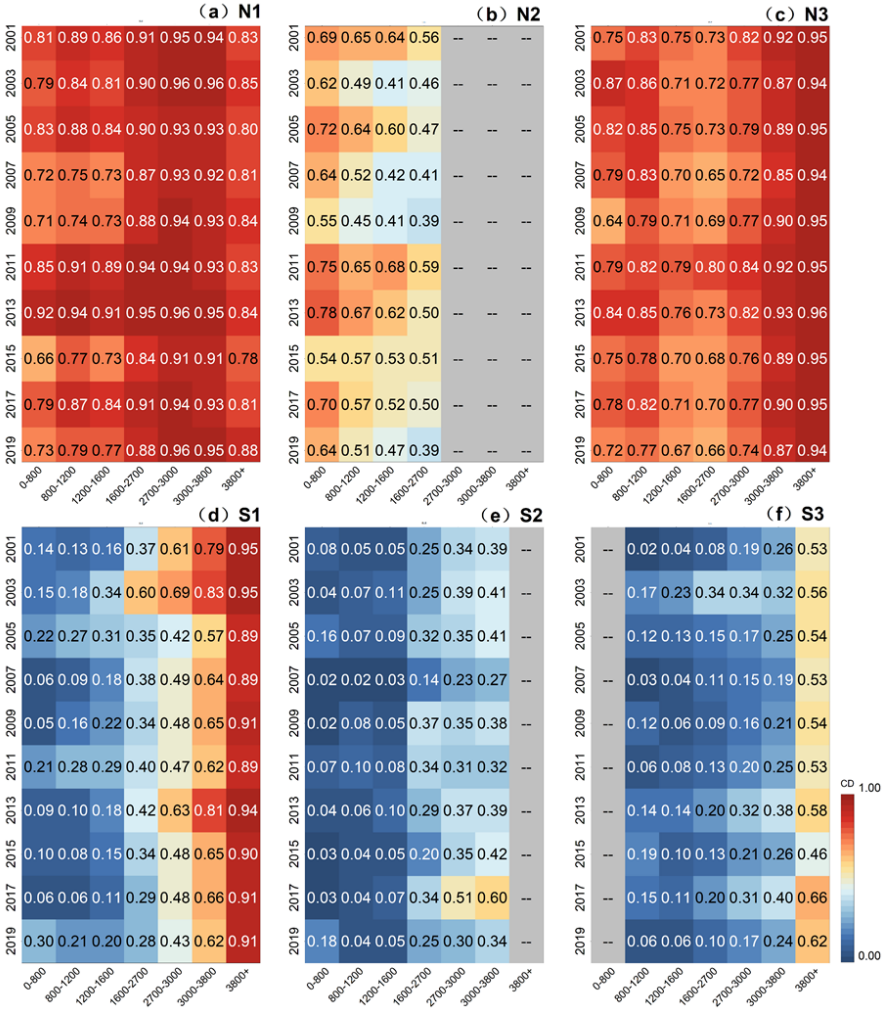

Figure 5. Annual Variations of SD-LST CD Across Different Altitude Over 20 Years

The most pronounced altitudinal increases in CD occur in the western Tianshan (S1) and Kunlun Mountains (S3), where values rise steeply from approximately 0.1 at lower elevations to nearly 1.0 in S1 and to around 0.6 in S3. In contrast, the Junggar Basin (N2) shows an inverse pattern, with CD generally ranging between 0.4–0.75 but decreasing with elevation. In the snow-scarce Tarim Basin (S2), overall CD remains low; however, a slight yet consistent positive correlation with altitude is observed. These altitudinal profiles highlight that the sensitivity of snow–temperature coupling to elevation varies substantially across different topographic and climatic settings, reinforcing the role of local environmental controls in modulating interaction strength.

https://doi.org/10.5194/egusphere-2026-1603
Preprint. Discussion started: 18 May 2026

4.2.2 Coupling Coordination Dynamics Between SD and LST

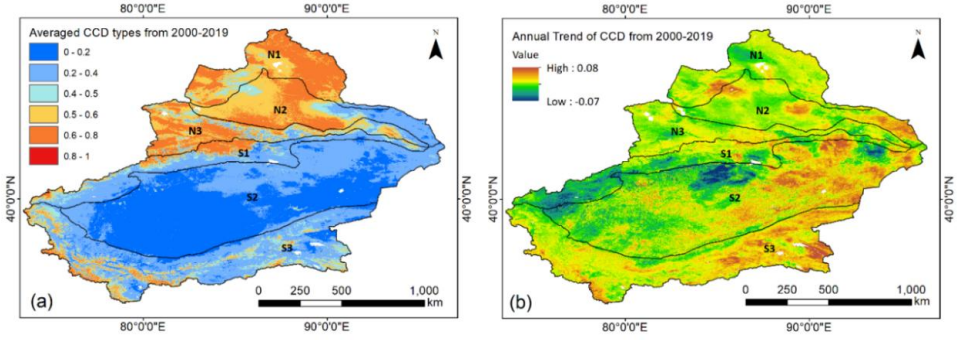

Figure 6. Distribution of average annual SD-LST CCD types (see Table 1 for type definitions) and their 20-year changing trends, with (a) showing type distribution and (b) showing changing trends.

The spatial distribution of the 20-year mean coupling coordination degree (CCD) for the SD–LST system is shown in Fig. 6a. No areas within Xinjiang were classified under the High-Quality Coordination category during the study period. In northern Xinjiang (N1, N2, N3), CCD values are generally higher, dominated by Primary Coordination and Critical Coordination, though localized zones of Near-Maladjustment and Moderate-Maladjustment are present. In contrast, southern Xinjiang exhibits markedly lower coordination: S1 and S3 are primarily classified as Primary Coordination with interspersed areas of Moderate-Maladjustment, while most of the Tarim Basin (S2) falls under Severe-Maladjustment. Overall, the SD–LST interaction in northern Xinjiang tends toward coordinated states, whereas southern Xinjiang is characterized by varying degrees of maladjustment.

Spatiotemporal trends in CCD over the 20-year period are presented in Fig. 6b. Although regional mean trends are generally weak, notable spatial heterogeneity in CCD change is evident. Within the major mountain systems, distinct patterns emerge: the Altai Mountains (N1) show relatively stable CCD, whereas significant differences occur between the northern and southern Tianshan ranges. The western subregion of N3 exhibits a statistically significant declining trend in CCD, while the Kunlun Mountains (S3) show a pronounced increasing trend. These results indicate that, over the study period, the strongest and most improving coordination occurred in the Kunlun Mountains, followed by the Altai and northern Tianshan regions, whereas the southern and western Tianshan Mountains experienced a tendency toward declining coordination, reflecting spatially divergent SD–LST synergies across Xinjiang's complex topography.

https://doi.org/10.5194/egusphere-2026-1603
Preprint. Discussion started: 18 May 2026

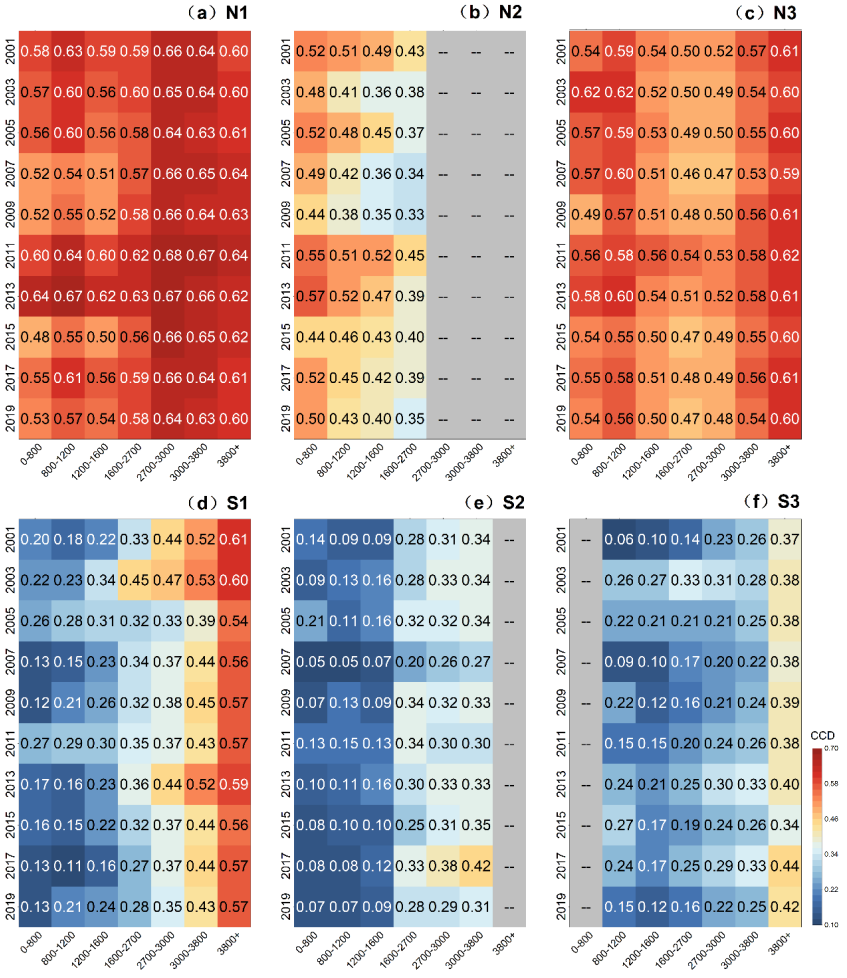

Figure 7. Annual Variations of SD-LST CCD Across Different Elevations Over 20 Years

Figure 7 illustrates the 20-year evolution of the SD–LST coupling coordination degree (CCD) across elevation gradients in Xinjiang, highlighting significant regional disparities. In the N1 region (Altai Mountains), CCD shows a positive correlation with elevation, peaking between 2700–3800 m, while declining gradually in the lower zone (0–1600 m). Conversely, in the N2 region (northern Tianshan), where snow is primarily distributed below 2700 m, CCD exhibits a consistent negative relationship with altitude, accompanied by a uniform declining trend across all elevations over the study period. The N3 region (western Tianshan) follows a U-shaped altitudinal pattern, with CCD decreasing initially before increasing at higher elevations, yet it demonstrates overall temporal stability. In southern Xinjiang (S1, S2, S3), CCD increases markedly with elevation, yet the temporal trends diverge: S1 and S2 display a slight annual decline, while S3 (Kunlun Mountains) shows a gradual strengthening over time. These patterns indicate that although elevation exerts a dominant control on coordination strength in southern Xinjiang, the temporal evolution of SD–LST synergy varies regionally, with the Kunlun Mountains exhibiting the most pronounced resilience against coordination loss.

https://doi.org/10.5194/egusphere-2026-1603
Preprint. Discussion started: 18 May 2026

4.3 Spatiotemporal Patterns in the Lagged Response of LST to Snow Depth Changes

4.3.1 Overall Characteristics of the SD–LST Lag

The time-lagged correlation between SD and LST was quantified by identifying the specific lag (in days) at which their correlation reached a maximum or minimum. This lag period represents the statistically significant response time of SD to LST variation. A spatial assessment was conducted to examine the distribution of these lag days across seasons, with results categorized and mapped in Fig. 8.

Autumn (Fig. 8a): Snow cover was present except in the arid S2 region and eastern N2, where temperatures remain above freezing or wind-driven ablation prevails. The SD–LST lag time was typically 7–14 days across most of Xinjiang. Exceptions included: (1) central N2 and western S1, where lags shortened to 0–7 days, likely due to elevated terrain and shallow snow reducing thermal inertia; (2) southeastern S3, where similarly short lags resulted from enhanced solar radiation and patchy snow cover with lower albedo; and (3) localized areas in northern S3 near the Tarim Basin, which exhibited near-instantaneous (0-day) response under extremely arid, wind-compacted snow conditions.

Winter (Fig. 8b): Lag times increased significantly relative to autumn (mean = 12.6 ± 4.3 days), with greater spatial variability (coefficient of variation = 34.2%). In N1, N2, N3, and S1, a bimodal distribution emerged: 7–14-day lags dominated mid-elevations, while 14–22-day lags occurred at higher latitudes, reflecting a latitudinal gradient in snowpack thermal inertia. Within S2, lag times varied widely (0–22 days), influenced by topographic barriers and cold-air advection. S3 showed predominantly 7–14-day lags but exhibited a clear east–west contrast: eastern sectors consistently displayed shorter lags (0–7 days), likely due to higher afternoon solar radiation and differing synoptic cold-front frequencies.

Spring (Fig. 8c): A pronounced north–south gradient in lag days was observed, except in the largely snow-free S2 region. Lag duration generally increased from north to south. Notable patterns included: near-instantaneous response (0-day lag) across N2; shortening lags from 7–14 days in the north to 0 days in the south within N1 and S1; and an eastward extension of lags from 0–7 days to 7–14 days in N3. In S3, lags shortened from 7–14 days in the south to 0–7 days in the north, suggesting possible influences from precipitation or snow density gradients.

Summer (Fig. 8d): Snow persisted only in high-elevation zones of N1, N3, S1, and S3. Lag times within these areas ranged mainly between 0–14 days, with minimal latitudinal variation but a distinct longitudinal pattern: eastern sectors exhibited shorter lags (0–7 days), while western sectors showed longer delays (7–14 days), likely due to differences in topography, radiation regimes, or precipitation phase.

https://doi.org/10.5194/egusphere-2026-1603
Preprint. Discussion started: 18 May 2026

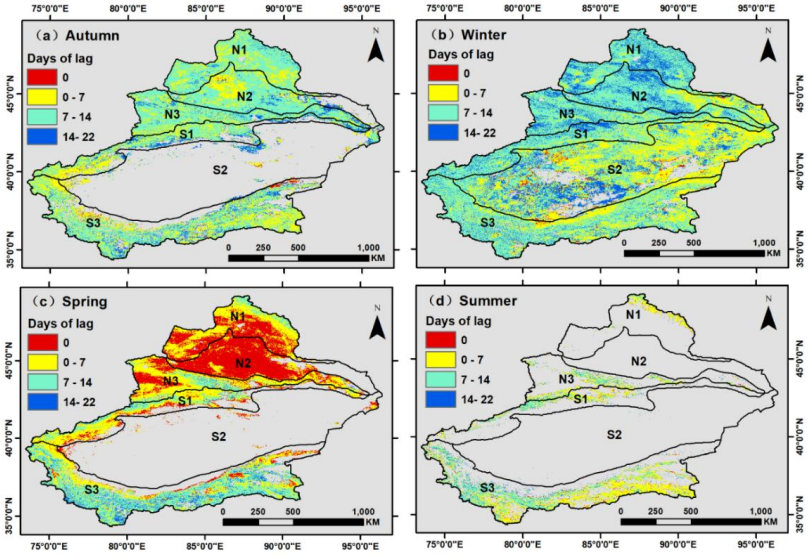

Figure 8. Spatial Distribution of Annual Average Lagged Time of SD to LST Across Different Seasons

4.3.2 Altitudinal and Seasonal Variability of SD–LST Lag Times

Figure 9 presents the seasonal statistics of lag duration between snow depth (SD) and land surface temperature (LST) across elevation zones in each sub-basin. The analysis reveals that both the mean lag and its altitudinal dependence undergo pronounced seasonal reversals and regional contrasts.

Autumn (Fig. 9a) was characterized by spatially homogeneous lag times (mean: 9 ± 1 days) and weak, regionally divergent altitudinal controls. While northern Xinjiang exhibited a unimodal relationship with elevation (peak at ~2500–3000 m), the southern basins (S1, S2) showed no systematic elevational trend. In contrast, the Kunlun Mountains (S3) displayed a strong, linear altitudinal increase (0.8–1.2 days/1000 m, $R^2 = 0.78$).

Winter (Fig. 9b) introduced a clear latitudinal gradient in mean lag (north: 11 ± 2 days; south: 9 ± 2.5 days) and a strengthening of average altitudinal variability (+20% compared to autumn). A fundamental north-south dichotomy emerged: northern basins showed a parabolic altitudinal pattern, whereas southern regions lacked a consistent elevational signal, despite a persistent positive correlation in S3.

Spring (Fig. 9c) exhibited the most extreme spatial heterogeneity. Mean lag spanned an order of magnitude from south to north (1 ± 0.5 to 9 ± 2 days), and altitudinal sensitivity reached its annual maximum (average within-basin variability: 11 ± 3 days). A near-universal positive lag-elevation relationship was observed across all sub-basins (1.5–2.5 days/500 m), steepest in the Tianshan Mountains. The bimodal elevational response in the Altay Mountains (N1) contrasted with the simpler linear patterns elsewhere.

Summer (Fig. 8d), with snow limited to alpine zones, revealed a striking east-west disparity in lag times (east: 0–7 days; west: 7–14 days) in the absence of a clear latitudinal gradient.

https://doi.org/10.5194/egusphere-2026-1603
Preprint. Discussion started: 18 May 2026

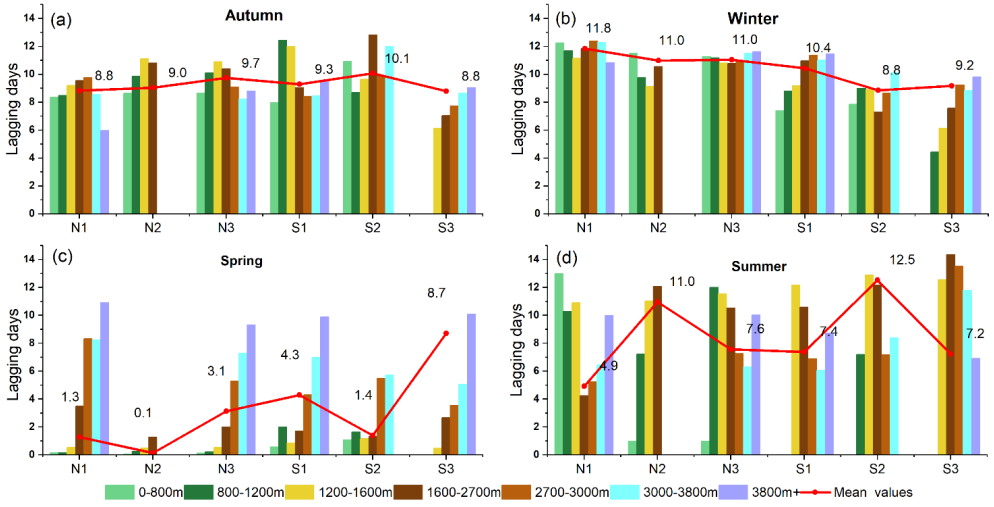

Figure 9. Seasonal Average Lagged Time of SD to LST in different elevations across sub-basins. (a) Autumn, (b) Winter, (c) Spring, (d) Summer.

4.3.3 Long-Term Trends in Seasonal Lag Times Across Mountain Regions

Long-term (2001–2020) trends in seasonal SD–LST lags reveal asynchronous regional trajectories across Xinjiang's Mountain regions, underscoring a seasonally divergent response to climate warming (Fig. 10). While some regions exhibit significant shifts in specific seasons, others remain stable, highlighting the distinct climatic and snowpack controls governing each mountain range.

Autumn Trends (Fig. 10a): Autumn lag times demonstrated the most pronounced long-term declines in the Tianshan regions. In the North Tianshan (N3), lags decreased from ~15 to 6 days (slope = −0.45 days/year, $p < 0.001$). A similar but less steep decline occurred in the South Tianshan (S1; from 11 to 8 days). The Altay Mountains (N1) showed high interannual variability (5–15 days) without a significant trend, while the Kunlun Mountains (S3) remained stable (8–10 days). These trends suggest a widespread acceleration of autumn snowpack response to cooling temperatures, particularly in the Tianshan.

Winter Trends (Fig. 10b): Winter lag times displayed region-specific patterns. The North Tianshan (N3) showed a significant decline from 15 to 11 days (slope = −0.20 days/year, $p < 0.01$). The South Tianshan (S1) maintained consistently higher lags than autumn (10–13 days after 2006) but without a clear trend. The Altay Mountains (N1) exhibited elevated lags during 2010–2015 (8–15 days), possibly linked to anomalous snowfall seasons. The Kunlun Mountains (S3) remained stable (8–10 days). The general reduction in winter lags, especially in the north, may reflect changes in snowpack structure or mid-winter melt events under warming winters.

Spring Trends (Fig. 10c): Lag times exhibited clear regional divergence. The Altay Mountains (N1) maintained stable, near-immediate responses (0–2 days). In contrast, both the North and South Tianshan (N3, S1) experienced significant lengthening of lags (N3: from ~2 to 5 days, slope = +0.15 days/year, $p < 0.01$; S1: from <4 to 8 days, slope = +0.20 days/year,

https://doi.org/10.5194/egusphere-2026-1603
Preprint. Discussion started: 18 May 2026

$p < 0.005$). The Kunlun Mountains (S3) displayed the highest absolute values (8–13 days) but a slight declining trend (−0.05 days/year). This pattern indicates that spring snowpack temperature sensitivity increased most markedly in the Tianshan system.

Summer Trends (Fig. 10d): Summer lag times showed moderate interannual variability without strong directional trends. The Altay (N1) and North Tianshan (N3) regions exhibited relative stability (N1: 4–8 days; N3: 7–11 days). The South Tianshan (S1) displayed greater fluctuation (6–10 days) and a slight overall decline (−0.03 days/year, $p = 0.12$). In the Kunlun Mountains (S3), summer lags were the most stable (7–9 days). The increased variability in N1 after 2010 suggests a possible shift in late-season snowpack stability or ablation energy sources.

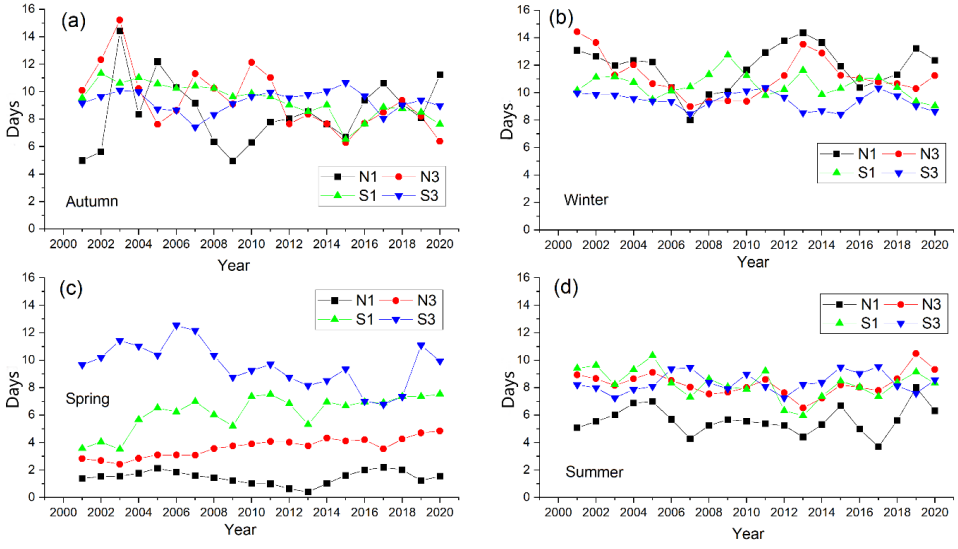

Figure 10. Long-term (2001–2020) trends in seasonal SD–LST response lags across four mountain regions in Xinjiang. (a) Autumn, (b) Winter, (c) Spring, (d) Summer.

5 Discussion

5.1. Hierarchical Controls on Snow–Temperature Interactions

Our analysis reveals that the spatial patterns of snow–temperature interactions across Xinjiang are governed by a coherent hierarchical control framework (Fig. 11), which is distinctly expressed through the unique climatic and cryospheric characteristics of its three major mountain systems: the Altay (N1), Tianshan (N3, S1), and Kunlun (S3). This integration of scale-dependent controls and regional specificity provides a mechanistic understanding of the observed heterogeneity.

At the macro-scale, the fundamental contrast between the cold-humid north and the hyper-arid south establishes the baseline potential for strong snow–temperature coupling(Sato, 2005). This is most clearly manifested in the Altay Mountains (N1), where abundant snowfall and a long snow season create a deep, persistent snowpack. This system operates under climate-dominated control, resulting in the highest and most stable coupling degrees observed, alongside the longest winter response

https://doi.org/10.5194/egusphere-2026-1603
Preprint. Discussion started: 18 May 2026

lags—a signature of high thermal inertia. This pattern aligns with stable seasonal snow–climate feedbacks typical of high-latitude regions. The Tianshan Mountains straddle this macro-gradient, with its northern slopes (N3) extending the humid-influenced regime and its southern slopes (S1) transitioning toward aridity.

The meso-scale control of elevation and topography modifies or even overrides the macro-scale template, particularly in the drier southern regions(Pepin et al., 2015). In the Kunlun Mountains (S3), elevation becomes the dominant, overriding control. The robust correlation between altitude and both coupling and coordination degrees illustrates a strict elevation-gating mechanism: only above a critical altitude (~3500 m) does a sufficiently persistent snowpack exist to establish a coordinated relationship with temperature. In the Tianshan Mountains, topography manifests as a sharp intra-mountain contrast. The pronounced north–south asymmetry in coupling and coordination is a direct result of the rain-shadow effect and differential solar radiation, making the south slope (S1) a more sensitive and vulnerable subsystem. Here, topography amplifies the macro-climatic gradient, creating strong internal heterogeneity.

The hierarchical controls are further mediated by micro-scale factors and seasonal dynamics, which are clearly captured in our time-lag and seasonal-stage analyses. This is evidenced by two key findings: (1) the systematic east–west divergence in response lags across regions, and (2) the shift in dominant thermal drivers across different stages of the ablation season (e.g., a change in the primary driver between early and peak ablation periods). Most importantly, the contrasting long-term trends—such as the significant lengthening of spring lags in the Tianshan versus the improving coordination in the Kunlun—demonstrate that system components are responding to climate change asynchronously, a behavior dictated by their unique position within this multi-scale framework.

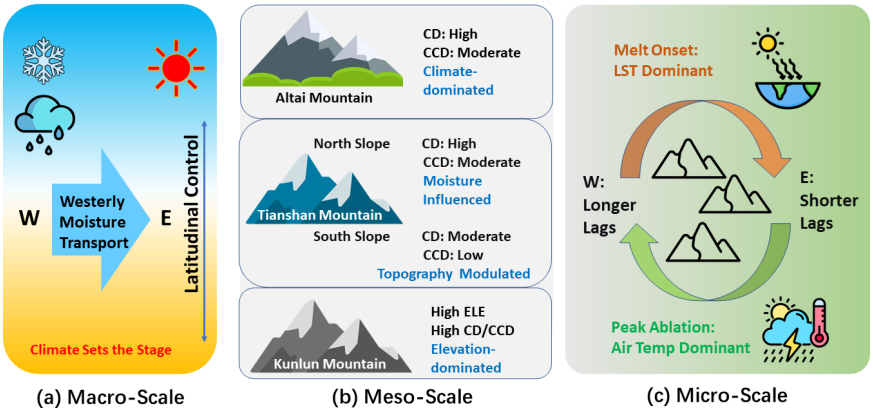

Figure 11. Hierarchical Controls on Snow–Temperature Interactions (a) Macro-scale: Climatic gradient setting. (b) Meso-scale: Climate/Topographic/Elevation modulation. (c) Micro-Scale: Seasonal ablation dynamics.

5.2. Decoupling Between Interaction Strength and System Harmony in Xinjiang

A high Coupling Degree (CD) reflects a strong statistical interdependence between snow depth (SD) and land surface

https://doi.org/10.5194/egusphere-2026-1603
Preprint. Discussion started: 18 May 2026

temperature (LST), serving as a quantitative indicator of efficient energy exchange at the snow–atmosphere interface. This is characteristic of thermally responsive snowpacks, as evidenced in our results by the consistently high CD values in the snow-rich Altay Mountains (N1) and the high-elevation zones of the Kunlun Mountains (S3).

However, our analysis reveals a critical and more nuanced insight: a high CD does not guarantee a high Coupling Coordination Degree (CCD). The CCD assesses the synchrony and sustainability of the co-evolution. The spatial mismatch between CD and CCD across Xinjiang provides a powerful diagnostic for ecosystem stress. Most notably, regions like the southern slopes of the Tianshan Mountains (S1) and parts of the northern Tianshan (N3) exhibit moderate-to-high CD but concurrently low or declining CCD. This “coupling-coordination decoupling” signals a system in dysfunction: while temperature remains a dominant driver of snowpack changes (hence high CD), the rate and nature of these changes are becoming maladaptive, undermining the system's harmonious state(Hantel and Hirtl-Wielke, 2007).

Several mechanisms, inferred from our spatiotemporal patterns, may explain this decoupling: (1) Loss of Buffering Capacity and Destructive Feedback: Exemplified by the high-CD, low-CCD state in low-elevation Southern Tianshan, thinning snowpacks lose thermal inertia and latent heat capacity. Spring warming thus triggers rapid ablation rather than gradual melt. While LST still directly drives this retreat (sustaining high CD), the resultant snow-cover collapse disrupts system harmony, marking a shift of snow from a climate moderator to a change amplifier(Shengdi et al., 2023). (2) Asynchronous Response Rates: The observed decline in CCD despite high CD suggests that the rate of LST increase may outpace stabilizing feedbacks. The snow-albedo feedback, a known positive feedback, likely exacerbates this asynchrony by accelerating warming once melt begins(Flanner et al., 2011). (3) Seasonal Shift in Interaction Mechanisms: Pronounced seasonal lag patterns, particularly the significant lengthening of spring lags, indicate a change in energy processing. Early ablation is likely directly driven by surface heating (short lags), while peak ablation may involve energy storage within the snowpack or other fluxes (e.g., net radiation), introducing greater delays(Wei et al., 2014). This intra-seasonal shift can maintain a high seasonal CD while degrading the synchrony essential for high CCD. The CD-CCD discrepancy is not an analytical artifact but a meaningful indicator. It moves the assessment beyond whether temperature drives snow changes, to evaluate how healthily the snow-climate system is co-evolving. Identifying regions with this decoupling (e.g., Southern Tianshan) highlights areas most vulnerable to rapid, potentially irreversible change under continued warming.

5.3. Lagged Responses as Indicators of Snowpack Thermal Inertia and Regional Heterogeneity

The response lag serves as a direct metric of snowpack thermal inertia, reflecting how efficiently energy perturbations propagate through the snow column. The pronounced spatiotemporal heterogeneity in lag times across Xinjiang is fundamentally shaped by regional differences in snowpack characteristics—governed by distinct climatic regimes—and reveals divergent system vulnerabilities.

In the Altay Mountains region (N1), the cold-humid continental climate coupling with abundant winter snowfall sustains

https://doi.org/10.5194/egusphere-2026-1603
Preprint. Discussion started: 18 May 2026

a deep seasonal snowpack characterized by high cold content. This results in the longest and most stable winter response lags observed across the study area (14–22 days), serving as a direct manifestation of its strong thermal inertia. The minimal interannual variation in these seasonal lags further indicates that snowpack depth and cold content remain the dominant controls, effectively buffering the system against abrupt shifts in melt timing. This high-inertia regime corresponds closely with the region's consistently high coupling coordination, reflecting a resilient snow–climate system in which temperature forcing and snowpack response remain in a state of relative equilibrium.

The Tianshan Mountains (N3 & S1) display a pronounced north–south asymmetry in lag patterns, which originates from fundamentally contrasting snowpack regimes(Lie-qun et al., 2013). Influenced by greater moisture availability, the northern slopes maintain a moderately deep and seasonally persistent snowpack, resulting in intermediate yet stable lag times. In contrast, the southern slopes experience a warmer and drier climatic regime, supporting only a shallower, more intermittently distributed snow cover. Notably, the significant lengthening of spring lags observed on the south slope suggests a possible increase in snowpack cold content—potentially linked to enhanced winter accumulation at higher elevations—or a shift in the dominant spring melt energy from sensible to radiative heating, a process that requires more time to offset the snowpack's energy deficit. This evolving dynamic indicates that the south slope is undergoing a regime transition, wherein its already limited snowpack is growing more sensitive to variations in winter precipitation and spring radiative forcing, thereby intensifying the coupling-coordination stress documented across this region.

Under hyper-arid climatic conditions, the snowpack in the Kunlun Mountains (S3) is sparse, shallow, and exhibits strong elevation dependence. At lower elevations, snow cover is transient, resulting in near-zero lag times. Only above approximately 3500 m does a thin yet seasonally persistent snowpack develop, displaying measurable lag responses. The relatively stable seasonal lags, coupling with an observed improvement in coordination, indicate that at these highest elevations the snowpack has attained a fragile yet stable equilibrium with the extreme environment. The existing snow depth is just sufficient to provide the necessary thermal inertia and sustain coordinated thermal exchange; however, any further warming or aridification could push the system below the persistence threshold, leading to rapid decoupling.

These regional patterns underscore that lag dynamics are not merely statistical outcomes but are emergent properties of snowpack structure under specific climatic forcing. The Altay's deep snow provides robust buffering, the Tianshan's asymmetric snowpack leads to divergent sensitivity, and the Kunlun's marginal snow exhibits threshold-dependent behavior. The lengthening spring lags in the Tianshan south slope are particularly telling: they indicate a system where changes in snow accumulation or melt energy are altering the fundamental timing of hydrological response, potentially increasing the risk of abrupt meltwater release. This regional synthesis clarifies that "one-size-fits-all" models of snow–temperature interaction are inadequate; future projections must account for these intrinsically different snowpack regimes and their unique lag-response sensitivities to climate change.

https://doi.org/10.5194/egusphere-2026-1603
Preprint. Discussion started: 18 May 2026

6 Conclusions

This study developed an integrated analytical framework combining the Coupling Coordination Degree Model (CCDM) with time-lagged correlation analysis to quantify snow depth–land surface temperature interactions across Xinjiang's complex mountain–basin systems. By moving beyond conventional statistical correlation, this framework enabled a multi-dimensional assessment of interaction strength, system harmony, and dynamic response characteristics.

We demonstrate that snow–temperature interactions are governed by a three-tiered hierarchical control system: macro-scale latitudinal climate gradients establish the baseline coupling potential; meso-scale elevation and topography modify or override this template, with elevation acting as a strict gatekeeper in the Kunlun and topographic asymmetry creating sharp intra-mountain contrasts in the Tianshan; and micro-scale local factors and seasonal dynamics further modulate response lags and energy exchange pathways.

Critically, we reveal that coupling degree and coordination degree are distinct diagnostic metrics. Their spatial mismatch—most pronounced in the southern Tianshan—serves as an early warning signal of system stress, identifying regions where rapid warming outpaces the snowpack's adaptive capacity. Response lag time is further established as a physically meaningful metric of snowpack thermal inertia and memory, with region-specific signatures ranging from the Altay's stable, long-duration lags (14–22 days) to the Kunlun's elevation-threshold-dependent behavior.

Divergent long-term trends (2001–2020)—autumn lag shortening, spring lag lengthening, and asynchronous regional trajectories—underscore that climate change impacts on mountain cryosphere are seasonally differentiated and regionally heterogeneous, precluding "one-size-fits-all" modeling approaches.

The CD-CCD-lag triad provides a transferable analytical framework applicable to other snow-dominated regions facing similar data-scarce, topographically complex conditions. By bridging statistical correlation and mechanistic understanding, this work supplies empirically derived parameters to improve snow–climate feedback representation in land surface and hydrological models. For Xinjiang and analogous arid mountain regions, the identified vulnerability (southern Tianshan) and resilience (Kunlun high-elevation zones) hotspots provide a scientific basis for prioritizing monitoring and climate adaptation strategies.

Future research should integrate process-based snowpack modeling to explicitly attribute observed patterns to specific energy balance components, and extend this framework to other Central Asian mountain ranges to advance continental-scale understanding of cryosphere–climate–hydrology interactions under accelerating warming.

data availability. Our snow depth dataset and land surface temperature dataset are available on http://www.ncdc.ac.cn and https://data.tpdc.ac.cn/home.

https://doi.org/10.5194/egusphere-2026-1603
Preprint. Discussion started: 18 May 2026

Author contributions. Haixing Li* conceived the main innovative ideas and led the experiments. Xiaolong Bao, Shiqi Lu, Yi Chu, and Jun Lu participated in the experiments and manuscript writing. Mengge Xiao and Xuelei Lei contributed to the data processing.

Competing interests. The authors declare an absence of competing interests.

Acknowledgements.

This research was supported by the Xinjiang Key Laboratory of Water Cycle and Utilization in Arid Zone under the funding project XJYS0907-2024-yb-03. The authors gratefully acknowledge the financial assistance provided by the laboratory.

References

Aizen, V. B., Aizen, E. M., and Kuzmichonok, V. A.: Glaciers and hydrological changes in the Tien Shan: simulation and prediction, Environ. Res. Lett., 2, 045019, 2007.

Arias, P., Bellouin, N., Coppola, E., Jones, R., Krinner, G., Marotzke, J., Naik, V., Palmer, M., Plattner, G.-K., and Rogelj, J.: Climate Change 2021: the physical science basis. Contribution of Working Group I to the Sixth Assessment Report of the Intergovernmental Panel on Climate Change; technical summary, 2021.

Barnett, T. P., Adam, J. C., and Lettenmaier, D. P.: Potential impacts of a warming climate on water availability in snow-dominated regions, Nature, 438, 303–309, 2005.

Beniston, M., Farinotti, D., Stoffel, M., Andreassen, L. M., Coppola, E., Eckert, N., Fantini, A., Giacona, F., Hauck, C., and Huss, M.: The European mountain cryosphere: a review of its current state, trends, and future challenges, The Cryosphere, 12, 759–794, 2018.

Chen, Y., Li, Z., Fan, Y., Wang, H., and Deng, H.: Progress and prospects of climate change impacts on hydrology in the arid region of northwest China, Environ. Res., 139, 11–19, 2015.

Clark, M. P., Hendrikx, J., Slater, A. G., Kavetski, D., Anderson, B., Cullen, N. J., Kerr, T., Örn Hreinsson, E., and Woods, R. A.: Representing spatial variability of snow water equivalent in hydrologic and land-surface models: A review, Water Resour. Res., 47, 2011WR010745, https://doi.org/10.1029/2011WR010745, 2011.

Essery, R.: Large-scale simulations of snow albedo masking by forests, Geophys. Res. Lett., 40, 5521–5525, https://doi.org/10.1002/grl.51008, 2013.

Flanner, M. G., Shell, K. M., Barlage, M., Perovich, D. K., and Tschudi, M. A.: Radiative forcing and albedo feedback from the Northern Hemisphere cryosphere between 1979 and 2008, Nat. Geosci., 4, 151–155, 2011.

Hantel, M. and Hirtl-Wielke, L.: Sensitivity of Alpine snow cover to European temperature, Int. J. Climatol., 27, 1265–1275, https://doi.org/10.1002/joc.1472, 2007.

Hock, R. and Holmgren, B.: A distributed surface energy-balance model for complex topography and its application to Storglaciären, Sweden, J. Glaciol., 51, 25–36, 2005.

https://doi.org/10.5194/egusphere-2026-1603
Preprint. Discussion started: 18 May 2026

Hu, R. J.: Physical geography of the Tianshan Mountains in China, China Environ. Sci. Press Beijing, 264–273, 2004.

Huang, J., Na, Y., and Guo, Y.: Spatiotemporal characteristics and driving mechanism of the coupling coordination degree of urbanization and ecological environment in Kazakhstan, J. Geogr. Sci., 30, 1802–1824, https://doi.org/10.1007/s11442-020-1813-9, 2020.

Immerzeel, W. W., Van Beek, L. P. H., and Bierkens, M. F. P.: Climate Change Will Affect the Asian Water Towers, Science, 328, 1382–1385, https://doi.org/10.1126/science.1183188, 2010.

Lai, Z., Ge, D., Xia, H., Yue, Y., and Wang, Z.: Coupling coordination between environment, economy and tourism: A case study of China, PLoS One, 15, e0228426, 2020.

Lehning, M., Bartelt, P., Brown, B., Fierz, C., and Satyawali, P.: A physical SNOWPACK model for the Swiss avalanche warning: Part II. Snow microstructure, Cold Reg. Sci. Technol., 35, 147–167, 2002a.

Lehning, M., Bartelt, P., Brown, B., and Fierz, C.: A physical SNOWPACK model for the Swiss avalanche warning: Part III: Meteorological forcing, thin layer formation and evaluation, Cold Reg. Sci. Technol., 35, 169–184, 2002b.

Li, H., Liu, J., Lei, X., Ju, Y., Bu, X., and Li, H.: Quantitative determination of environmental factors governing the snow melting: a geodetector case study in the central Tienshan Mountains, Sci. Rep., 12, 11565, 2022.

Li, Y., Chen, Y., and Li, Z.: Climate and topographic controls on snow phenology dynamics in the Tienshan Mountains, Central Asia, Atmospheric Res., 236, 104813, 2020.

Lie-qun, H. U., Shuai, L., and Feng-chao, L.: Analysis of the variation characteristics of snow covers in Xinjiang region during recent 50 years, J. Glaciol. Geocryol., 35, 793–800, 2013.

Liston, G. E. and Elder, K.: A distributed snow-evolution modeling system (SnowModel), J. Hydrometeorol., 7, 1259–1276, 2006.

Liu, Y. B., Li, R. D., and Song, X. F.: Grey associative analysis of regional urbanization and eco-environment coupling in China, Acta Geogr. Sin., 60, 237–247, 2005.

López-Moreno, J. I., Pomeroy, J. W., Revuelto, J., and Vicente-Serrano, S. M.: Response of snow processes to climate change: spatial variability in a small basin in the Spanish Pyrenees, Hydrol. Process., 27, 2637–2650, https://doi.org/10.1002/hyp.9408, 2013.

Male, D. H. and Gray, D. M.: Handbook of snow: Principles, processes, management & use, Pergamon Press, 1981.

Marchane, A., Jarlan, L., Hanich, L., Boudhar, A., Gascoin, S., Tavernier, A., Filali, N., Le Page, M., Hagolle, O., and Berjamy, B.: Assessment of daily MODIS snow cover products to monitor snow cover dynamics over the Moroccan Atlas mountain range, Remote Sens. Environ., 160, 72–86, 2015.

Marks, D. and Dozier, J.: Climate and energy exchange at the snow surface in the alpine region of the Sierra Nevada: 2. Snow cover energy balance, Water Resour. Res., 28, 3043–3054, 1992.

Marty, C., Schlögl, S., Bavay, M., and Lehning, M.: How much can we save? Impact of different emission scenarios on future snow cover in the Alps, The Cryosphere, 11, 517–529, 2017.

Meng, Q., Pi, H., Nie, Y., and Ma, J.: Research on the coupling and coordinated development of guangxi's tourism industry, new urbanization and environmental health system in the post-epidemic era, Front. Public Health, 12, 1331765, 2024.

https://doi.org/10.5194/egusphere-2026-1603
Preprint. Discussion started: 18 May 2026

Musselman, K. N., Clark, M. P., Liu, C., Ikeda, K., and Rasmussen, R.: Slower snowmelt in a warmer world, Nat. Clim. Change, 7, 214–219, 2017.

Nijssen, B., O'Donnell, G. M., Hamlet, A. F., and Lettenmaier, D. P.: Hydrologic Sensitivity of Global Rivers to Climate Change, Clim. Change, 50, 143–175, https://doi.org/10.1023/A:1010616428763, 2001.

Pepin, N., Bradley, R., Diaz, H., Baraer, M., Caceres, E. B., Forsythe, N., Fowler, H., Greenwood, G., Hashmi, M. Z., and Liu, X. D.: Elevation-dependent warming in mountain regions of the world. Nature Clim Change, 5: 424–430, 2015.

Pomeroy, J. W., Gray, D. M., Shook, K. R., Toth, B., Essery, R. L. H., Pietroniro, A., and Hedstrom, N.: An evaluation of snow accumulation and ablation processes for land surface modelling, Hydrol. Process., 12, 2339–2367, https://doi.org/10.1002/(SICI)1099-1085(199812)12:15%253C2339::AID-HYP800%253E3.0.CO;2-L, 1998.

Raleigh, M. S., Lundquist, J. D., and Clark, M. P.: Exploring the impact of forcing error characteristics on physically based snow simulations within a global sensitivity analysis framework, Hydrol. Earth Syst. Sci., 19, 3153–3179, 2015.

Sato, T.: The TianShan rain-shadow influence on the arid climate formation in northwestern China, Sola, 1, 13–16, 2005.

Shengdi, W., Bin, C. A. O., Jiansheng, H. A. O., Wen, S. U. N., and Zhiwei, Z.: Effects of seasonal snow cover on ground surface temperature in Xinjiang, J. Glaciol. Geocryol., 45, 435–445, 2023.

Smith, R. B. and Barstad, I.: A linear theory of orographic precipitation, J. Atmospheric Sci., 61, 1377–1391, 2004.

Song, C. Q., Cheng, C. X., Yang, X. F., Ye, S. J., and Gao, P. C.: Understanding geographic coupling and achieving geographic integration, Acta Geogr. Sin., 75, 3–13, 2020.

Wang, H., Zhang, X., Xiao, P., Zhang, K., and Wu, S.: Elevation-dependent response of snow phenology to climate change from a remote sensing perspective: A case survey in the central Tianshan Mountains from 2000 to 2019, Int. J. Climatol., 42, 1706–1722, 2022.

Wasserman, L.: All of Statistics: A Concise Course in Statistical Inference, Springer New York, New York, NY, https://doi.org/10.1007/978-0-387-21736-9, 2004.

Wei, Z., Yongping, S., Jianqiao, H., Bin, H. E., Hazaizi, N., Xuejiao, W. U., and Guoya, W.: Snow properties on different underlying surfaces during snow-melting period in the Altay Mountains: Observation and analysis, J. Glaciol. Geocryol., 36, 491–499, 2014.

Xuezhi, F., Wenjun, L. I., and Yanchen, B. A. I.: Research on the methods of obtaining satellite snow cover information, JournalofImage Graph., 5, 836–839, 2000.

Zhang, X., Li, X., Li, L., Zhang, S., and Qin, Q.: Environmental factors influencing snowfall and snowfall prediction in the Tianshan Mountains, Northwest China, J. Arid Land, 11, 15–28, https://doi.org/10.1007/s40333-018-0110-2, 2019.

Zhang, Y., Fang, Z., and Xie, Z.: Study on the coupling coordination between ecological environment and high-quality economic development in urban agglomerations in the middle reaches of the Yangtze River, Int. J. Environ. Res. Public. Health, 20, 3612, 2023.

Zhao, W., Ni, Z., Yin, C., Liu, Y., and Pereira, P.: Research framework for integrated geography: Composite driving–system evolution–coupling mechanism–synergistic regulation, Geogr. Sustain., 6, 100321, 2025.